Allele-specific silencing of dominant disease genes

Victor M. Miller*†, Haibin Xia‡, Ginger L. Marrs*†, Cynthia M. Gouvion*, Gloria Lee‡, Beverly L. Davidson*†‡§, and Henry L. Paulson*†¶

*Department of Neurology, †Graduate Program in Genetics, and Departments of ‡Internal Medicine and §Physiology and Biophysics, University of Iowa Roy J. and Lucille A. Carver College of Medicine, Iowa City, IA 52242

Edited by Charles M. Radding, Yale University School of Medicine, New Haven, CT, and approved April 9, 2003 (received for review February 17, 2003)

Small interfering RNA (siRNA) holds therapeutic promise for silencing dominantly acting disease genes, particularly if mutant alleles can be targeted selectively. In mammalian cell models we demonstrate that allele-specific silencing of disease genes with siRNA can be achieved by targeting either a linked single-nucleotide polymorphism (SNP) or the disease mutation directly. For a polyglutamine neurodegenerative disorder in which we first determined that selective targeting of the disease-causing CAG repeat is not possible, we took advantage of an associated SNP to generate siRNA that exclusively silenced the mutant Machado–Joseph disease/spinocerebellar ataxia type 3 allele while sparing expression of the WT allele. Allele-specific suppression was accomplished with all three approaches currently used to deliver siRNA: *in vitro*-synthesized duplexes as well as plasmid and viral expression of short hairpin RNA. We further optimized siRNA to specifically target a missense Tau mutation, V337M, that causes frontotemporal dementia. These studies establish that siRNA can be engineered to silence disease genes differing by a single nucleotide and highlight a key role for SNPs in extending the utility of siRNA in dominantly inherited disorders.

Modulation of gene expression by endogenous, noncoding RNAs is increasingly appreciated to play a role in eukaryotic development, maintenance of chromatin structure, and genomic integrity (1). Recently, techniques have been developed to trigger RNA interference (RNAi) against specific targets in mammalian cells by introducing exogenously produced or intracellularly expressed small interfering RNAs (siRNAs) (2, 3). These methods have proven to be quick, inexpensive, and effective for knockdown experiments *in vitro* and *in vivo* (2–5). The ability to accomplish selective gene silencing has led to the hypothesis that siRNAs might be used to suppress gene expression for therapeutic benefit (5–7).

Dominantly inherited diseases would seem to be ideal candidates for siRNA-based therapy. To explore the utility of siRNA in inherited human disorders, we used cellular models to test whether we could target mutant alleles causing two classes of dominantly inherited, untreatable neurodegenerative diseases: polyglutamine (polyQ) neurodegeneration in Machado–Joseph disease/spinocerebellar ataxia type 3 (MJD/SCA3) and frontotemporal dementia with parkinsonism linked to chromosome 17 (FTDP-17). The polyQ neurodegenerative disorders consist of at least nine diseases caused by CAG-repeat expansions that encode polyQ in the disease protein. polyQ expansion confers a dominant toxic property on the mutant protein that is associated with aberrant accumulation of the disease protein in neurons (8). In FTDP-17, Tau mutations lead to the formation of neurofibrillary tangles accompanied by neuronal dysfunction and degeneration (9, 10). The precise mechanisms by which these mutant proteins cause neuronal injury are unknown, but considerable evidence suggests that the abnormal proteins themselves initiate the pathogenic process (8). Accordingly, eliminating expression of the mutant protein by siRNA or other means, in principle, should slow or even prevent disease (11). However, because many dominant disease genes may also encode essential proteins (e.g., ref. 12), we sought to develop siRNA-mediated approaches that inactivate mutant alleles selectively while allowing continued expression of the WT protein.

Methods

siRNA Synthesis. *In vitro* siRNA synthesis has been described (13). Reactions were performed with desalted DNA oligonucleotides (Integrated DNA Technologies, Coralville, IA) and the AmpliScribeT7 high-yield transcription kit (Epicentre Technologies, Madison, WI). Yield was determined by absorbance at 260 nm. Annealed siRNAs were assessed for double-stranded character by agarose gel (1% wt/vol) electrophoresis and ethidium bromide staining. Note that for all siRNAs generated in this study, the most 5′ nucleotide in the targeted cDNA sequence is referred to as position 1 and each subsequent nucleotide is numbered in ascending order from 5′ to 3′.

Plasmid Construction. The human ataxin-3 cDNA was expanded to 166 CAGs by PCR (14). PCR products were digested at *Bam*HI and *Kpn*I sites introduced during PCR and ligated into *Bgl*II and *Kpn*I sites of pEGFP-N1 (CLONTECH), resulting in full-length expanded ataxin-3 fused to the N terminus of enhanced GFP (EGFP). Untagged ataxin-3-Q166 was constructed by ligating a *Ppu*MI–*Not*I ataxin-3 fragment (3′ of the CAG repeat) into ataxin-3-Q166-GFP cut with *Ppu*MI and *Not*I to remove EGFP and replace the normal ataxin-3 stop codon. Ataxin-3-Q28-GFP was generated as described above from pcDNA3.1-ataxin-3-Q28. Constructs were sequence-verified to ensure that no PCR mutations were present. Expression was verified by Western blot with anti-ataxin-3 (15) and GFP antibodies (Medical and Biological Laboratories, Nagoya, Japan). The construct encoding a flag-tagged, 352-residue Tau isoform has been described (16). The pEGFP-Tau plasmid was constructed by ligating the human Tau cDNA into pEGFP-C2 (CLONTECH) and encodes Tau with EGFP fused to the N terminus. The pEGFP-TauV337M plasmid was derived by using site-directed mutagenesis (QuikChange kit, Stratagene) of the pEFGP-Tau plasmid.

Cell Culture and Transfections. Culture of Cos-7 and HeLa cells has been described (17). Transfections with plasmids and siRNA were performed by using Lipofectamine Plus (Invitrogen) according to the manufacturer's instructions. For ataxin-3 expression, 1.5 μg of plasmid was transfected with 5 μg of *in vitro*-synthesized siRNAs. For Tau experiments, 1 μg of plasmid was transfected with 2.5 μg of siRNA. For expression of hairpin siRNA from the phU6 constructs, 1 μg of ataxin-3 expression plasmid was transfected with 4 μg of phU6-siC10i or phU6-siG10i. Cos-7 cells infected with siRNA-expressing adenovirus were transfected with 0.5 μg of each expression plasmid.

Stably transfected, doxycycline-inducible cell lines were generated in a subclone of PC12 cells, PC6-3, because of its strong neural differentiation properties (18). A PC6-3 clone stably

This paper was submitted directly (Track II) to the PNAS office.

Abbreviations: RNAi, RNA interference; siRNA, small interfering RNA; polyQ, polyglutamine; MJD/SCA3, Machado–Joseph disease/spinocerebellar ataxia type 3; FTDP-17, frontotemporal dementia with parkinsonism linked to chromosome 17; EGFP, enhanced GFP; shRNA, short hairpin RNA; siMiss, mistargeted siRNA; RFP, red fluorescent protein; SNP, single-nucleotide polymorphism.

¶To whom correspondence should be addressed at: Department of Neurology, University of Iowa Roy J. and Lucille A. Carver College of Medicine, 2007 RCP, Iowa City, IA 52242. E-mail: henry-paulson@uiowa.edu.

GENETICS

expressing Tet repressor plasmid (provided by S. Strack, University of Iowa) was transfected with pcDNA5/TO-ataxin-3(Q28) or pcDNA5/TO-ataxin-3(Q166) (Invitrogen). After selection in hygromycin, clones were characterized by Western blot and immunofluorescence. Two clones, PC6-3-ataxin3(Q28)#33 and PC6-3-ataxin3(Q166)#41, were chosen because of their tightly inducible, robust expression of ataxin-3.

siRNA Plasmid and Viral Production. Plasmids expressing ataxin-3 short hairpin RNAs (shRNAs) were generated by insertion of head-to-head 21-bp hairpins in phU6 that corresponded to siC10 and siG10 (5).

Recombinant adenovirus expressing ataxin-3-specific shRNA was generated from phU6-C10i (encoding C10 hairpin siRNA) and phU6si-G10i (encoding G10 hairpin siRNA) as described (5, 19).

Western Blotting and Immunofluorescence. Cos-7 cells expressing ataxin-3 were harvested 24–48 h after transfection (17). Stably transfected, inducible cell lines were harvested 72 h after infection with adenovirus. Lysates were assessed for ataxin-3 expression by Western blot analysis as described (17) with polyclonal rabbit anti-ataxin-3 antisera at a 1:15,000 dilution or 1C2 antibody specific for expanded polyQ tracts (20) at a 1:2,500 dilution. Cells expressing Tau were harvested 24 h after transfection. Protein was detected with an affinity-purified polyclonal antibody to a human Tau peptide (residues 12–24) at a 1:500 dilution. Anti-α-tubulin mouse monoclonal antibody (Sigma) was used at a 1:10,000 dilution, and GAPDH mouse monoclonal antibody (Sigma) was used at a 1:1,000 dilution.

Immunofluorescence for ataxin-3 (17) was carried out by using 1C2 antibody (Chemicon) at a 1:1,000 dilution 48 h after transfection. Flag-tagged, WT Tau was detected by using mouse monoclonal antibody (Sigma) at a 1:1,000 dilution 24 h after transfection. Both proteins were detected with rhodamine-conjugated secondary antibody at a 1:1,000 dilution.

Fluorescent Imaging and Quantification. Fixed samples were observed with a Zeiss Axioplan fluorescence microscope. Digital images were collected on separate red, green, and blue fluorescence channels by using a SPOT digital camera. Images were assembled and overlaid by using PHOTOSHOP 6.0 (Adobe Systems, Mountain View, CA). Live cell images were collected with a Kodak MDS 290 digital camera mounted to an Olympus (Tokyo) CK40 inverted microscope. Fluorescence was quantitated by collecting three nonoverlapping images per well at low power ($\times$10). Pixel count and intensity for each image were determined by using NOVA PRIME software (BIOQUANT Image Analysis, Nashville, TN). Background was subtracted by quantitation of images from cells of equivalent density under identical fluorescent illumination. Mock-transfected cells were used to assess background fluorescence for all experiments and were stained with appropriate primary and secondary antibodies for simulated heterozygous experiments. Average fluorescence is reported from two to three independent experiments. The mean of two to three independent experiments for cells transfected with the indicated expression plasmid and a mistargeted siRNA (siMiss) was set at 1. Error bars depict variation between experiments as the standard error of the mean. In simulated heterozygous experiments, a blinded observer scored cells with a positive fluorescence signal for expression of WT, mutant, or both proteins in random fields at high power for two independent experiments. More than 100 cells were scored in each experiment and reported as the number of cells with coexpression divided by the total number of transfected cells.

Table 1. Primers for generation of *in vitro*-synthesized siRNA

Name	Primer sequence (5′–3′)
Ataxin-3	
siMiss	CGGCAAGCTGCGCATGAAGTTC
	ATGAACTTCATGCTCAGCTTGC
siGFP	ATGAACTTCAGGGTCAGCTTGC
	CGGCAAGCTGACCCTGAAGTTC
siC7	CAGCAGCGGGACCTATCAGGAC
	CTGTCCTGATAGGTCCCGCTGC
siG10	CAGCAGCAGGGGGACCTATC
	CTGATAGGTCCCCCTGCTGC
siC7/8	CAGCAGCCGGACCTATCAGGAC
	CTGTCCTGATAGGTCCGGCTGC
siC10	CAGCAGCAGCGGGACCTATC
	CTGATAGGTCCCGCTGCTGC
siN′CAG	TTGAAAAACAGCAGCAAAAGC
	CTGCTTTTGCTGCTGTTTTTC
siCAG	CAGCAGCAGCAGCAGCAGCAGC
	CTGCTGCTGCTGCTGCTGCTGC
Tau	
siN′-Tau	TCGAAGTGATGGAAGATCACGC
	CAGCGTGATCTTCCATCACTTC
si272	CAGCCGGGAGTCGGGAAGGTGC
	CTGCACCTTCCCGACTCCCGGC
si301	ACGTCCTCGGCGGCGGCAGTGTGC
	TTGCACACTGCCGCCTCCGCGGAC
si406	ACGTCTCCATGGCATCTCAGC
	TTGCTGAGATGCCATGGAGAC
siA9	GTGGCCAGATGGAAGTAAAATC
	CAGATTTTACTTCCATCTGGCC
siA9/C8	GTGGCCACATGGAAGTAAAATC
	CAGATTTTACTTCCATGTGGCC
siA9/C12	GTGGCCAGATGCAAGTAAAATC
	CAGATTTTACTTGCATCTGGCC

Primer sequences for *in vitro* synthesis of siRNAs using T7 polymerase are shown. All primers contain the T7 promoter sequence 5′-TATAGTGAGTCGTATTA-3′ at their 3′ ends. The primer 5′-TAATACGACTCACTATAG-3′ was annealed to all oligos to synthesize siRNAs.

Results

Direct Silencing of Expanded Alleles. We first attempted suppression of mutant polyQ expression using siRNA complementary to the CAG repeat and immediately adjacent sequences to determine whether the expanded repeat differentially altered the susceptibility of the mutant allele to siRNA inhibition (Table 1). We transfected HeLa cells with various *in vitro*-synthesized siRNAs (13) and plasmids encoding normal or expanded polyQ fused to red fluorescent protein (RFP) or GFP, respectively (Q19-RFP and Q80-GFP) (Fig. 1*a*). In negative control cells transfected with Q80-GFP, Q19-RFP, and siMiss, Q80-GFP formed aggregates (21) that recruited the normally diffuse Q19-RFP (Fig. 1*a*). When the experiment was performed with siRNA targeted to GFP as a positive control for allele-specific silencing, Q80-GFP expression was nearly abolished, whereas Q19-RFP continued to be expressed as a diffusely distributed protein (Fig. 1*a*). When Q19-RFP and Q80-GFP were cotransfected with siRNA directly targeting the CAG repeat (siCAG) (Fig. 1*a*) or an immediately adjacent 5′ region (data not shown), expression of both proteins was suppressed efficiently.

To test whether siRNA could selectively silence expression of a full-length polyQ disease protein, we designed siRNAs that target the transcript encoding ataxin-3, the disease protein in MJD, also known as SCA3 (8) (Fig. 1*b*). In transfected cells, siRNA directed against three separate regions, the CAG repeat, a distant 5′ site, or a site just 5′ to the CAG repeat (siN′CAG),

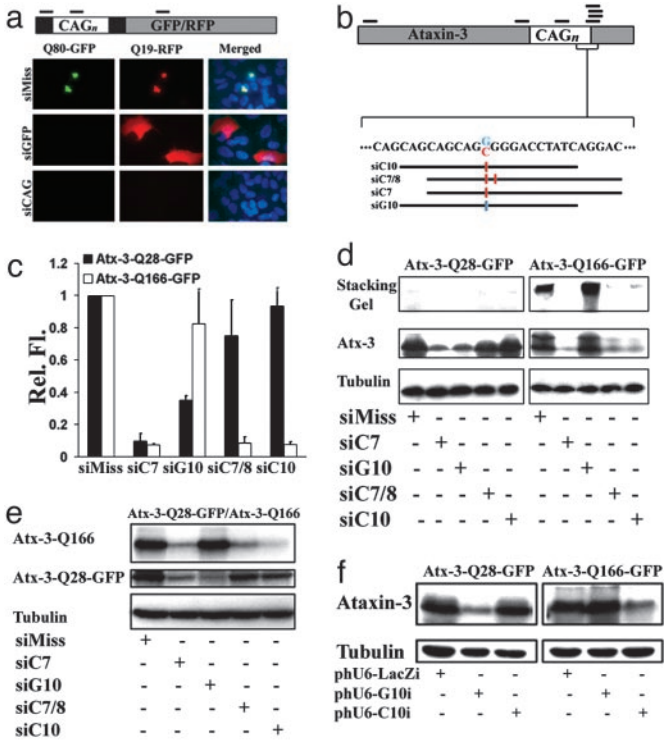

Fig. 1. RNAi-mediated suppression of expanded CAG repeat-containing genes. Expanded CAG repeats are not direct targets for preferential inactivation (*a*), but a linked SNP can be exploited to generate siRNA that selectively silences mutant ataxin-3 expression (*b–f*). (*a*) Schematic of cDNA encoding generalized polyQ-fluorescent protein fusions. The bars indicate regions targeted by siRNAs. HeLa cells cotransfected with Q80-GFP, Q19-RFP, and the indicated siRNA. Nuclei are visualized by 4′,6-diamidino-2-phenylindole staining (blue) in merged images. (*b*) Schematic of human ataxin-3 cDNA, with bars indicating regions targeted by siRNAs. The targeted SNP (G987C) is shown in color. In the displayed siRNAs, red or blue bars denote C or G, respectively. (*c*) Quantitation of fluorescence in Cos-7 cells transfected with WT or mutant ataxin-3 (Atx)-GFP expression plasmids and the indicated siRNA. Fluorescence from cells cotransfected with siMiss was set at 1. The bars depict mean total fluorescence from three independent experiments ± SEM. Rel. Fl., relative fluorescence. (*d*) Western blot analysis of cells cotransfected with the indicated ataxin-3 expression plasmids (*Upper*) and siRNAs (*Lower*). Appearance of aggregated, mutant ataxin-3 in the stacking gel (seen with siMiss and siG10) is prevented by siRNA inhibition of the mutant allele. (*e*) Allele specificity is retained in the simulated heterozygous state. Western blot analysis of Cos-7 cells cotransfected with WT (Atx-3-Q28-GFP) and mutant (Atx-Q166) expression plasmids along with the indicated siRNAs (mutant ataxin-3 detected with 1C2, an antibody specific for expanded polyQ, and WT ataxin-3 detected with anti-ataxin-3 antibody). (*f*) Western blot of Cos-7 cells transfected with ataxin-3-GFP expression plasmids and plasmids encoding the indicated shRNA. The negative control plasmid, phU6-LacZi, encodes siRNA specific for LacZ. Both normal and mutant proteins were detected with anti-ataxin-3 antibody. Tubulin immunostaining is shown as a loading control in *d–f*.

resulted in efficient but not allele-specific suppression of ataxin-3 containing normal or expanded repeats (data not shown). Consistent with an earlier study with longer double-stranded RNA (22), our results suggest that expanded CAG repeats and adjacent sequences, although accessible to RNAi, are not preferential targets for silencing.

Allele-Specific Silencing of the Mutant polyQ Gene in MJD/SCA3. In further efforts to selectively inactivate the mutant allele we took advantage of a single nucleotide polymorphism (SNP) in the *MJD1* gene, a G-to-C transition immediately 3′ to the CAG repeat (G987C) (Fig. 1*b*). This SNP is in linkage disequilibrium with the disease-causing expansion, in most families segregating perfectly with the disease allele. Worldwide, 70% of disease chromosomes carry the C variant (23). Our ataxin-3 expression cassettes, which were generated from patients (15), contain the C variant in all expanded ataxin-3 constructs and the G variant in all normal ataxin-3 constructs. To test whether this G-to-C mismatch could be distinguished by siRNA, we designed siRNAs that included the last two CAG triplets of the repeat followed by the C variant at position 7 (siC7) (Table 1 and Fig. 1*b*), resulting in a perfect match only for expanded alleles. Despite the presence of a single mismatch to the WT allele, siC7 strongly inhibited expression of both alleles (Fig. 1 *c* and *d*). We then introduced a second G-to-C mismatch at position 8 such that the siRNA now contained two mismatches to WT and only one to mutant alleles (siC7/8). The siC7/8 siRNA effectively suppressed mutant ataxin-3 expression, reducing total fluorescence to an average of 8.6% of control levels, with only modest effects on WT ataxin-3 (average 75.2% of control). siC7/8 also nearly eliminated the accumulation of aggregated mutant ataxin-3, a pathological hallmark of disease (24) (Fig. 1*d*).

To optimize differential suppression, we designed siRNAs containing a more centrally placed mismatch. Because the center of the antisense strand directs cleavage of target mRNA in the RNA-induced silencing complex (25), we reasoned that central mismatches might discriminate between WT and mutant alleles more efficiently. We designed siRNAs that place the C of the SNP at position 10 (siC10), preceded by the final three triplets in the CAG repeat (Table 1 and Fig. 1*b*). In transfected cells, siC10 caused allele-specific suppression of the mutant protein (Fig. 1 *c* and *d*). Fluorescence from expanded ataxin-3-Q166-GFP was reduced dramatically (7.4% of control levels), whereas fluorescence of ataxin-3-Q28-GFP showed minimal change (93.6% of control) (Fig. 1 *c* and *d*). Conversely, siRNA engineered to suppress only the WT allele (siG10) inhibited WT expression with little effect on expression of the mutant allele (Fig. 1 *c* and *d*). Importantly, inclusion of three CAG repeats at the 5′ end of the siRNA did not inhibit expression of Q19-GFP, Q80-GFP, or full-length ataxin-1-Q30, proteins that each are encoded by CAG repeat-containing transcripts (Fig. 5, which is published as supporting information on the PNAS web site, www.pnas.org).

In the disease state, normal and mutant alleles are expressed simultaneously. In plants and worms, activation of RNAi against one transcript results in the spread of silencing signals to other targets due to RNA-dependent RNA polymerase activity primed by the introduced RNA (26, 27). Although spreading has not been detected in mammalian cells and RNA-dependent RNA polymerase activity is not required for effective siRNA inhibition (28–30), most studies have used cell-free systems in which a mammalian RNA-dependent RNA polymerase could have been inactivated. If triggering the mammalian RNAi pathway against one allele activates cellular mechanisms that also silence the other allele, then siRNA applications might be limited to nonessential genes. To test this possibility, we simulated the heterozygous state by cotransfecting ataxin-3-Q28-GFP and ataxin-3-Q166 and analyzing suppression by Western blot. As shown in Fig. 1*e*, each siRNA retained the specificity observed in separate transfections: siC7 inhibited both alleles, siG10 inhibited only the WT allele, and siC7/8 and siC10 inhibited only mutant allele expression.

Effective siRNA therapy for late-onset disease likely will require sustained intracellular expression of the siRNA. Accordingly, we extended our experiments to two intracellular methods of siRNA production and delivery: expression plasmids and recombinant virus (3, 5). We constructed plasmids expressing siG10 or siC10 siRNA from the human U6 promoter as a hairpin transcript that is processed intracellularly to produce siRNA (3, 5). When cotransfected with ataxin-3-GFP expression plasmids, phU6-G10i and phU6-C10i-siRNA plasmids specifically suppressed WT or mutant ataxin-3 expression, respectively (Fig. 1*f*).

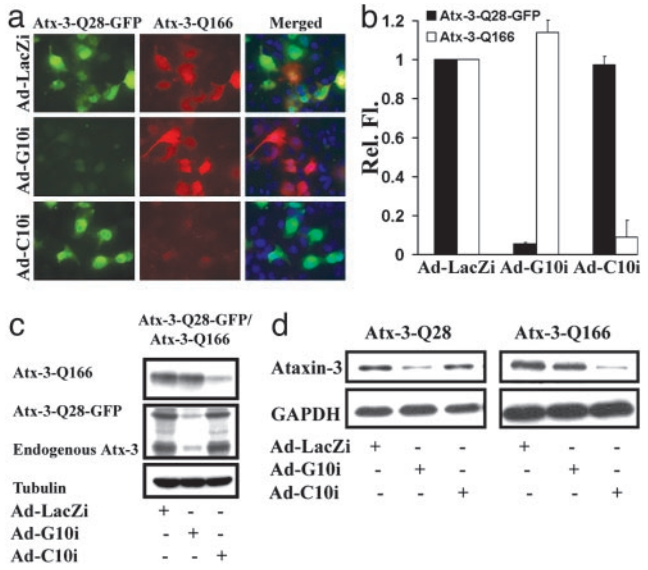

Fig. 2. shRNA-expressing adenovirus mediates allele-specific silencing in transiently transfected Cos-7 cells simulating the heterozygous state. (*a*) Representative images of cells cotransfected to express WT and mutant ataxin (Atx)-3 and infected with the indicated adenovirus (Ad) at 50 multiplicities of infection. Ataxin-3-Q28-GFP (green) is directly visualized, and ataxin-3-Q166 (red) is detected by immunofluorescence with the 1C2 antibody. Nuclei visualized with 4′,6-diamidino-2-phenylindole staining in merged images. An average of 73.1% of cells coexpressed both ataxin-3 proteins with Ad-LacZi. (*b*) Quantitation of mean fluorescence from two independent experiments was performed as described for *a*. Rel. Fl., relative fluorescence. (*c*) Western blot analysis of viral-mediated silencing in Cos-7 cells expressing WT and mutant ataxin-3 as described for *a*. Shown are mutant ataxin-3 detected with 1C2 antibody and WT human and endogenous primate ataxin-3 detected with anti-ataxin-3 antibody. (*d*) shRNA-expressing adenovirus mediates allele-specific silencing in stably transfected neural cell lines. Differentiated PC12 neural cells expressing WT (*Left*) or mutant (*Right*) ataxin-3 were infected with adenovirus (100 multiplicities of infection) engineered to express the indicated hairpin siRNA. Shown are Western blots immunostained for ataxin-3 and GAPDH as loading control.

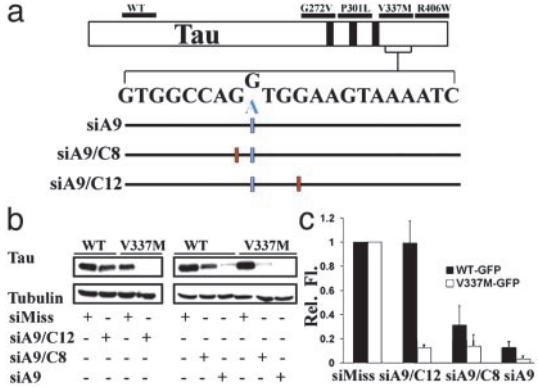

Fig. 3. Allele-specific siRNA suppression of a missense Tau mutation. (*a*) Schematic of human Tau cDNA with bars indicating regions and mutations tested for siRNA suppression. Of these, the V337M region showed effective suppression and was studied further. Vertical bars represent microtubule-binding repeat elements in Tau. In the displayed siRNAs, blue and red bars denote A and C, respectively. (*b*) Western blot analysis of cells cotransfected with WT or V337M Tau-EGFP fusion proteins and the indicated siRNAs. Cells were lysed 24 h after transfection and probed with anti-Tau antibody. Tubulin immunostaining is shown as a loading control. (*c*) Quantitation of fluorescence in Cos-7 cells transfected with WT Tau-EGFP or mutant V337M Tau-EGFP expression plasmids and the indicated siRNAs. The bars depict mean fluorescence and SEM from three independent experiments. Fluorescence from cells cotransfected with siMiss was set at 1. Rel. Fl., relative fluorescence.

This result encouraged us to engineer recombinant adenoviral vectors expressing allele-specific siRNA (5). We tested viral-mediated suppression in Cos-7 cells transiently transfected with both ataxin-3-Q28-GFP and ataxin-3-Q166 to simulate the heterozygous state. In Cos-7 cells infected with adenovirus encoding siG10, siC10, or negative control siRNA (Ad-G10i, Ad-C10i, and Ad-LacZi, respectively), we observed allele-specific silencing of WT ataxin-3 expression with Ad-G10i and of mutant ataxin-3 with Ad-C10i (Fig. 2 *a–c*). Quantitation of fluorescence (Fig. 2*b*) showed that Ad-G10i reduced WT ataxin-3 to 5.4% of control levels, whereas mutant ataxin-3 expression remained unchanged. Conversely, Ad-C10i reduced mutant ataxin-3 fluorescence levels to 8.8% of control and retained 97.4% of WT signal. These results were confirmed by Western blot, with which we further observed that Ad-G10i virus decreased endogenous (primate) ataxin-3, whereas Ad-C10i did not (Fig. 2*c*). A BLAST search of the nonredundant database revealed that in all available primate ataxin-3 sequences (including gorilla, chimp, and macaque species) a G nucleotide is conserved at the first position immediately 3′ to the CAG repeat.

We also assessed viral-mediated suppression in differentiated PC12 neural cell lines that inducibly express normal (Q28) or expanded (Q166) mutant ataxin-3. After infection with Ad-G10i, Ad-C10i, or Ad-LacZi, differentiated neural cells were placed in doxycycline for 3 days to induce maximal expression of ataxin-3. Western blot analysis of cell lysates confirmed that the Ad-G10i virus suppressed only WT ataxin-3, Ad-C10i virus suppressed only mutant ataxin-3, and Ad-LacZi had no effect on either normal or mutant ataxin-3 expression (Fig. 2*d*). Thus, we have established that siRNA retains its efficacy and selectivity across different modes of production and delivery to achieve allele-specific silencing of ataxin-3.

Allele-Specific Silencing of a Missense Tau Mutation. The preceding results indicate that, for DNA-repeat mutations in which the repeat itself does not present an effective target, an associated SNP can be exploited to achieve allele-specific silencing. To test whether siRNA works equally well to silence disease-causing mutations directly, we targeted missense Tau mutations that cause FTDP-17 (9, 10). A series of 21- to 24-nt siRNAs were generated *in vitro* against four missense FTDP-17 mutations: G272V, P301L, V337M, and R406W (Table 1 and Fig. 3*a*). In each case the point mutation was placed centrally, near the likely cleavage site in the RNA-induced silencing complex (position 9, 10, or 11) (14). A fifth siRNA designed to target a 5′ sequence in all Tau transcripts was also tested. To screen for siRNA-mediated suppression, we cotransfected GFP fusions of mutant and WT Tau isoforms together with siRNA into Cos-7 cells. Of the five targeted sites, we only obtained robust suppression with siRNA corresponding to V337M (Table 1 and Fig. 3*a*) (9, 10) and thus focused further analysis on this mutation. The V337M mutation is a G-to-A base change in the first position of the codon (GTG to ATG), and the corresponding V337M siRNA contains the A missense change at position 9 (siA9). This intended V337M-specific siRNA preferentially silenced the mutant allele but also caused significant suppression of WT Tau (Fig. 3 *b* and *c*). Based on the success of our approach with ataxin-3, we designed two additional siRNAs that contained the V337M (G-to-A) mutation at position 9 as well as a second introduced G-to-C mismatch immediately 5′ to the mutation (siA9/C8) or three nucleotides 3′ to the mutation (siA9/C12) such that the siRNA now contained two mismatches to the WT but only one to the mutant allele. This strategy resulted in further preferential inactivation of the mutant allele. One siRNA, siA9/C12, showed strong selectivity for the mutant Tau allele, reducing fluorescence to 12.7% of control levels without detect-

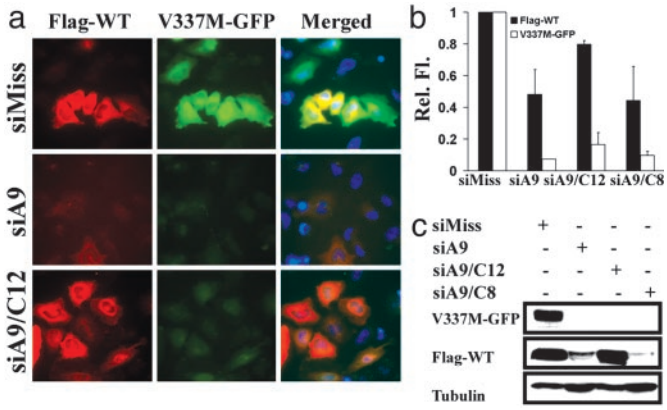

Fig. 4. Allele-specific silencing of Tau in cells simulating the heterozygous state. (*a*) Representative fluorescent images of fixed HeLa cells cotransfected with flag-tagged WT-Tau (red), V337M-Tau-GFP (green), and the indicated siRNAs. An average of 73.7% of cells coexpressed both Tau proteins with siMiss. Although siA9 suppresses both alleles, siA9/C12 selectively decreased expression of mutant Tau only. Nuclei were visualized with 4′,6-diamidino-2-phenylindole stain in merged images. (*b*) Quantitation of mean fluorescence from two independent experiments was performed as described for *a*. Rel. Fl., relative fluorescence. (*c*) Western blot analysis of cells cotransfected with flag-tagged WT-Tau and V337M-Tau-EGFP fusion proteins and the indicated siRNAs. Cells were lysed 24 h after transfection and probed with an anti-Tau antibody. V337M-GFP Tau was differentiated on the basis of reduced electrophoretic mobility due to the addition of GFP. Tubulin immunostaining is shown as a loading control.

able loss of WT Tau (Fig. 3 *b* and *c*). Next, we simulated the heterozygous state by cotransfecting V337M-GFP and flag-tagged WT-Tau expression plasmids (Fig. 4). In cotransfected HeLa cells, siA9/C12 silenced the mutant allele (16.7% of control levels) with minimal alteration of WT expression assessed by fluorescence (Fig. 4*a*) and Western blot (Fig. 4*b*). In addition, siA9 and siA9/C8 displayed better allele discrimination than we had observed in separate transfections but continued to suppress both WT and mutant Tau expression (Fig. 4).

Discussion

Despite the rapidly growing siRNA literature, questions remain concerning the design and application of siRNA both as a research tool and a therapeutic strategy. Our study, demonstrating allele-specific silencing of dominant disease genes, sheds light on important aspects of both applications.

Because many disease genes encode essential proteins, development of strategies to exclusively inactivate mutant alleles is important for the general application of siRNA to dominant diseases. Our results for two unrelated disease genes demonstrate that in mammalian cells it is possible to silence a single disease allele without activating pathways analogous to those found in plants and worms that result in the spread of silencing signals (26, 27). Although this result might have been predicted by the absence of RNA-dependent RNA polymerase homologs in the mouse and human genomes (31) and by data showing that siRNAs act as guides rather than primers in the mammalian RNAi pathway (29), our findings provide experimental evidence that such spreading is unlikely to complicate allele-specific silencing in mammalian systems. Neither RNA duplexes nor shRNA seemed to trigger significant spreading of RNAi in our experiments. Based on our findings, we conclude that allele-specific silencing should be possible for many dominant disease genes. Issues of *in vivo* delivery and efficacy remain to be resolved, of course. Notably, the long-term consequences of chronically triggering the RNAi pathway *in vivo*, as may be required to treat neurodegenerative conditions, are unknown.

Our data indicate that genes can differ widely in their susceptibility to inhibition, with no obvious sequence features predicting the success or failure of a given siRNA. For example, every siRNA we designed against ataxin-3 displayed significant activity (7/7, 100%), whereas Tau proved more difficult to inhibit, with only a single region centered on the V337M mutation yielding effective siRNAs (3/7, 43%). Moreover, although silencing of a specific gene is readily achieved once an accessible target is found, preferential silencing of a particular allele of that gene requires careful design and engineering of the siRNA. Our results indicate, for example, that a single nucleotide difference between two alleles may not be sufficient to confer allele specificity unless it is placed centrally in the siRNA, which suggests that at least two factors contribute to siRNA specificity: (*i*) the overall efficiency of base-pairing between siRNA and mRNA and (*ii*) the presence of Watson–Crick base-pairing between siRNA and mRNA at the central position across from the RNA-induced silencing complex cleavage site. In this study we have demonstrated that these factors can be manipulated by introducing peripheral mismatches to alter the silencing specificity of siRNA. Beginning with simply and economically prepared RNA duplexes, we have shown that multiple targets and siRNA designs can be screened systematically to optimize allele-specific siRNA for a disease gene. Once the best siRNA has been identified by this approach, it can be incorporated into shRNA expressed from plasmids or viral vectors that retain the efficacy and allele specificity of the original duplex.

In summary, we conclude that siRNA can be engineered to silence expression of disease alleles differing from WT alleles by as little as a single nucleotide. We have established that this approach can target missense mutations directly, as in frontotemporal dementia, or associated SNPs, as in MJD/SCA3. Our stepwise strategy for optimizing allele-specific targeting, together with recent advances in viral delivery (5) and the demonstration of RNAi in primary neurons (32), should extend the utility of siRNA to a wide range of dominant diseases in which the disease gene normally plays an important or essential role. One such example is another polyQ disease, Huntington disease (HD), in which normal HD protein levels are developmentally essential (12). The availability of mouse models for many dominant disorders including MJD/SCA3 (33), HD (34), and FTDP-17 (35) should speed the *in vivo* testing of siRNA-based therapy for these and other human diseases.

We thank Stefan Strack for the PC6-3 Tet repressor cell line and John Donelson for providing RFP. This work was supported by National Institutes of Health Predoctoral Training Grant T32 GM08629 (to the University of Iowa program in genetics and V.M.M.) and National Institutes of Health Grants RO1 NS38712-04 (to H.L.P.) and RO1 HD044093-01 (to B.L.D. and H.L.P.).

1. McManus, M. T. & Sharp, P. A. (2002) *Nat. Rev. Genet.* **3,** 737–747.
2. Elbashir, S. M., Harborth, J., Lendeckel, W., Yalcin, A., Weber, K. & Tuschl, T. (2001) *Nature* **411,** 494–498.
3. Brummelkamp, T. R., Bernards, R. & Agami, R. (2002) *Science* **296,** 550–553.
4. McCaffrey, A. P., Meuse, L., Pham, T. T., Conklin, D. S., Hannon, G. J. & Kay, M. A. (2002) *Nature* **418,** 38–39.
5. Xia, H., Mao, Q., Paulson, H. L. & Davidson, B. L. (2002) *Nat. Biotechnol.* **20,** 1006–1010.
6. Jacque, J. M., Triques, K. & Stevenson, M. (2002) *Nature* **418,** 435–438.
7. Gitlin, L., Karelsky, S. & Andino, R. (2002) *Nature* **418,** 430–434.
8. Zoghbi, H. Y. & Orr, H. T. (2000) *Annu. Rev. Neurosci.* **23,** 217–247.
9. Poorkaj, P., Bird, T. D., Wijsman, E., Nemens, E., Garruto, R. M., Anderson, L., Andreadis, A., Wiederholt, W. C., Raskind, M. & Schellenberg, G. (1998) *Ann. Neurol.* **43,** 815–825.
10. Hutton, M., Lendon, C. L., Rizzu, P., Baker, M., Froelich, S., Houlden, H., Pickering-Brown, S., Chakraverty, S., Isaacs, A., Grover, A., *et al.* (1998) *Nature* **393,** 702–705.
11. Yamamoto, A., Lucas, J. J. & Hen, R. (2000) *Cell* **101,** 57–66.

12. Nasir, J., Floresco, S. B., O'Kusky, J. R., Diewert, V. M., Richman, J. M., Zeisler, J., Borowski, A., Marth, J. D., Phillips, A. G. & Hayden, M. R. (1995) *Cell* **81,** 811–823.
13. Donze, O. & Picard, D. (2002) *Nucleic Acids Res.* **30,** e46.
14. Laccone, F., Maiwald, R. & Bingemann, S. (1999) *Hum. Mutat.* **13,** 497–502.
15. Paulson, H. L., Das, S. S., Crino, P. B., Perez, M. K., Patel, S. C., Gotsdiner, D., Fischbeck, K. H. & Pittman, R. N. (1997) *Ann. Neurol.* **41,** 453–462.
16. Leger, J. G., Brandt, R. & Lee, G. (1994) *J. Cell. Sci.* **107,** 3403–3412.
17. Chai, Y., Koppenhafer, S., Shoesmith, S., Perez, M. & Paulson, H. (1999) *Hum. Mol. Genet.* **8,** 673–682.
18. Pittman, R. N., Wang, S., DiBenedetto, A. J. & Mills, J. C. (1993) *J. Neurosci.* **13,** 3669–3680.
19. Anderson, R. D., Haskell, R. E., Xia, H., Roessler, B. J. & Davidson, B. L. (2000) *Gene Ther.* **7,** 1034–1038.
20. Trottier, Y., Lutz, Y., Stevanin, G., Imbert, G., Devys, D., Cancel, G., Saudou, F., Weber, C., David, G., Tora, L., *et al.* (1995) *Nature* **378,** 403–406.
21. Onodera, O., Burke, J. R., Miller, S. E., Hester, S., Tsuji, S., Roses, A. D. & Strittmatter, W. J. (1997) *Biochem. Biophys. Res. Commun.* **238,** 599–605.
22. Caplen, N. J., Taylor, J. P., Statham, V. S., Tanaka, F., Fire, A. & Morgan, R. A. (2002) *Hum. Mol. Genet.* **11,** 175–184.
23. Gaspar, C., Lopes-Cendes, I., Hayes, S., Goto, J., Arvidsson, K., Dias, A., Silveira, I., Maciel, P., Coutinho, P., Lima, *et al.* (2001) *Am. J. Hum. Genet.* **68,** 523–528.
24. Chan, H. Y., Warrick, J. M., Gray-Board, G. L., Paulson, H. L. & Bonini, N. M. (2000) *Hum. Mol. Genet.* **9,** 2811–2820.
25. Elbashir, S. M., Martinez, J., Patkaniowska, A., Lendeckel, W. & Tuschl, T. (2001) *EMBO J.* **20,** 6877–6888.
26. Fire, A., Xu, S., Montgomery, M. K., Kostas, S. A., Driver, S. E. & Mello, C. C. (1998) *Nature* **391,** 806–811.
27. Tang, G., Reinhart, B. J., Bartel, D. P. & Zamore, P. D. (2003) *Genes Dev.* **17,** 49–63.
28. Chiu, Y. L. & Rana, T. M. (2002) *Mol. Cell* **10,** 549–561.
29. Schwarz, D. S., Hutvagner, G., Haley, B. & Zamore, P. D. (2002) *Mol. Cell* **10,** 537–548.
30. Martinez, J., Patkaniowska, A., Urlaub, H., Luhrmann, R. & Tuschl, T. (2002) *Cell* **110,** 563–574.
31. Stein, P., Svoboda, P., Anger, M. & Schultz, R. M. (2003) *RNA* **9,** 187–192.
32. Krichevsky, A. M. & Kosik, K. S. (2002) *Proc. Natl. Acad. Sci. USA* **99,** 11926–11929.
33. Cemal, C. K., Carroll, C. J., Lawrence, L., Lowrie, M. B., Ruddle, P., Al-Mahdawi, S., King, R. H., Pook, M. A., Huxley, C. & Chamberlain, S. (2002) *Hum. Mol. Genet.* **11,** 1075–1094.
34. Lin, C. H., Tallaksen-Greene, S., Chien, W. M., Cearley, J. A., Jackson, W. S., Crouse, A. B., Ren, S., Li, X. J., Albin, R. L. & Detloff, P. J. (2001) *Hum. Mol. Genet.* **10,** 137–144.
35. Tanemura, K., Murayama, M., Akagi, T., Hashikawa, T., Tominaga, T., Ichikawa, M., Yamaguchi, H. & Takashima, A. (2002) *J. Neurosci.* **22,** 133–141.